［溶接学会論文集　第 33 巻　第 2 号　p. 39s-43s （2015）］

Investigation of Evaluation Method for Hot Cracking Susceptibility of 310S Stainless Steel during Laser Welding using Trans-Varestraint Test＊

Dan Wang,** Shuntaro Sakoda,** Kota Kadoi,*** Kenji Shinozaki,*** and Motomichi Yamamoto***

Solidification cracking occurs as a result of thermal strain and solidification behavior that is determined by welding conditions, especially welding speed. Brittle temperature range (BTR), an important index for evaluating solidification cracking, is used to quantity the effect of welding speed on susceptibility to solidification cracking. However, measurement of BTR using Trans-Varestraint test during laser welding has rarely been studied. The purpose of this work is to investigate the effect of welding speed on solidification cracking susceptibility in type 310S stainless steel using Trans-Varestraint test during laser welding. Solidification cracking and ductility-dip cracking were distinguished by observing fracture surfaces. Compared with traditional Trans-Varestraint test carried out for gas tungsten arc welding, the number of solidification cracks and total crack lengths during laser welding were lower; however, the number density of solidification cracks and total crack length per bead width during laser welding were higher. Both of these values had a tendency to first increase and then decrease slightly with increasing welding speed: the maximum values occurred at approximately 1.5 m/min. Temperature profiles at 0.2 and 1.0 m/min during laser welding were measured by an optical-fiber radiation thermometer combined with in-situ observation using a high-speed camera. BTR was measured using the center crack length along the heat flow in the welding direction. BTR at 1.0 m/min was less than that at 0.2 m/min during laser welding because the maximum crack length appeared at the side of molten pool at welding speeds greater than 1.0 m/min.

Key Words: Hot cracking susceptibility, Solidification cracking susceptibility, Trans-Varestraint test, Laser welding, In-situ observation

1. Introduction

Laser beam welding (LBW), owing to its high power, high efficiency, and ability to achieve high welding speeds and lower distortions, has been widely applied in industry. However, it is also well known that welding conditions, such as welding speed, are important in influencing solidification behavior and thermal strain that correspond to susceptibility to solidification cracking [1, 2]. Specifically, use of high welding speeds increases solidification cracking susceptibility [3].

Trans-Varestraint test during gas tungsten arc welding (GTAW) has been widely used to evaluate hot cracking susceptibility [4]. The number of cracks, crack length, and brittle temperature range (BTR) are measured as important indexes to evaluate hot cracking susceptibility. However, it is expected to be difficult to apply conventional evaluation methods, such as measurement of temperature profile, to Trans-Varestraint test during LBW because the cooling rate during LBW is much higher than that of GTAW. Although a few reports [5] have evaluated hot cracking susceptibility using Trans-Varestraint test during LBW, an appropriate method for this application is still under discussion.

In the present work, we investigate a method for evaluating applicability of Trans-Varestraint test during LBW and the effect of welding speed of LBW on hot cracking susceptibility.

* Received:
** Student Member, Graduate School of Engineering, Hiroshima University
*** Member, Graduate School of Engineering, Hiroshima University

2. Experimental procedure

Type 310S stainless steel, with a specimen size of 110 mm × 110 mm × 5 mm, was used. The chemical composition is shown in Table 1. Figure 1 shows the experimental setup for Trans-Varestraint test during LBW with in-situ observation using a high-speed camera. LBW conditions are shown in Table 2. A fiber laser was employed as the heat source. Welding speed was changed from 0.2 to 2.0 m/min. Laser power was adjusted to obtain half penetration in the thickness direction. Laser powers were 1.0 kW for 0.2 m/min, 1.85 kW for 1.0 m/min, 2.25 kW for 1.5 m/min, and 2.5 kW for 2.0 m/min. The laser spot size was 0.4 mm (just focus) and the laser head was tilted 25° to the welding direction to avoid interference by the high-speed camera. Ar gas was blown at 50 l/min onto the surface and rear of the specimen during LBW. For comparison, GTAW was also carried out, using a welding speed of 0.2 m/min, arc current of 180 A, arc length of 2 mm, torch tilting angle of 20°, and flow rate of Ar shielding gas of 20 l/min.

When the trailing edge of the molten pool moved to the center of specimen during LBW, bending strain was applied on the specimen as LBW stopped and hot cracking occurred. Augmented strain was measured using a strain gauge at room temperature, and the value was varied from 0.8 % to 4.3 % by using various surface radii of bending blocks. The cooling rate becomes quite high for Trans-Varestraint test during LBW at high welding speeds; therefore fast bending is required because initiation and propagation of the cracks have to be completed before the specimen solidifies completely. In this study, the testing machine and the fiber laser were accurately synchronized and a fast bending speed, approximately 350 mm/s (yoke movement), was applied.

The high-speed camera was set up vertically with the center of the specimen to capture the shape of the molten pool after hot cracking started. Laser lighting was used to provide brightness and image clarity. The number of cracks, crack lengths, and fracture surface were evaluated using scanning electron microscopy (SEM). Temperature profiles were measured by direct insertion of an optical-fiber radiation thermometer (ϕ 250 μm) with a high response rate into the rear of the molten pool during welding. The insertion position and time were monitored by the high-speed camera. The liquidus temperature was determined when the trailing edge of the molten pool reached the center of the fiber thermometer.

3. Results and discussion

Figure 2 shows hot cracking distributions after Trans-Varestraint test (augmented strain: 2.8%) during LBW at 0.2 m/min and 1.0 m/min. At 0.2 m/min, the shape of the molten pool backend is a smooth curve and the longest solidification crack (SC) initiates from the trailing edge of the rear center of the molten pool, similar to that in conventional GTAW [6]. However, at a welding speed of 1.0 m/min, the rear of the molten pool is teardrop-shaped. The higher welding speeds form more elongated shapes, from elliptical to teardrop, because of changes, such as the rate and the direction, in the heat flow conditions. Moreover, long SC and ductility-dip crack (DDC) tend to occur at the sides of the molten pool, compared with the rear of the molten pool, as shown in Fig. 2b. This tendency was also found at the higher welding speeds of 1.5 m/min and 2. 0 m/min.

To confirm the type of hot cracking, the fracture surface was investigated by opening the crack. Figure 3 shows a SEM image of the fracture surface of the longest crack obtained at 1.0 m/min (shown in Fig. 2b). On the high-temperature side, dendrite morphology is observed, as shown in Fig. 3a. Along the direction from the high- to low-temperature side, the dendrite arms become obscure and tiny hollows form, as shown in Figs. 3b and c. On

Table 1 Chemical composition of Type 310S (mass %).

C	Si	Mn	P	S	Ni	Cr	Co	Fe
0.04	0.43	0.96	0.019	0.001	20.13	25.19	0.09	Bal.

Table 2 Laser welding conditions.

Welding speed, m/min	0.2	1.0	1.5	2.0
Laser power, kW	1.0	1.85	2.25	2.5
Laser spot size, mm	0.4 (just focus)			
Laser irradiation angle, deg	25			
Ar shielding gas, l/min	50			

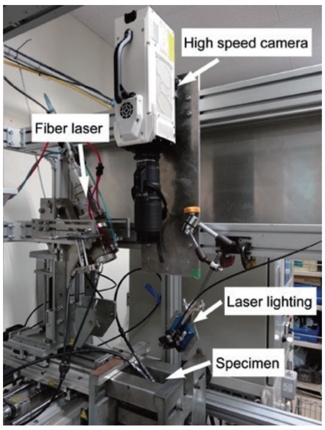

Fig. 1 Experimental setup of Trans-Varestraint test during LBW.

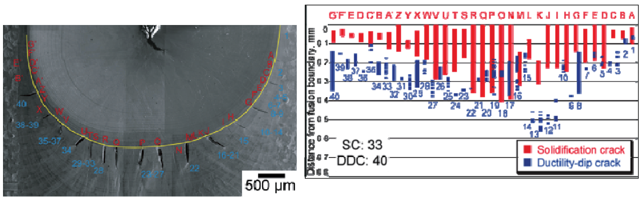

a) 0.2 m/min

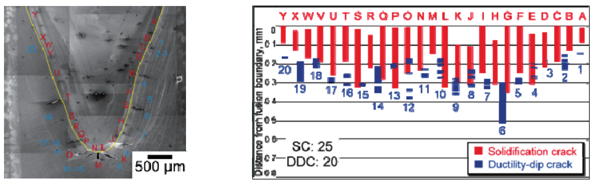

b) 1.0 m/min

Fig. 2 Distributions of SC and DDC during LBW at 0.2 and 1.0 m/min. (Augmented strain: 2.8%)

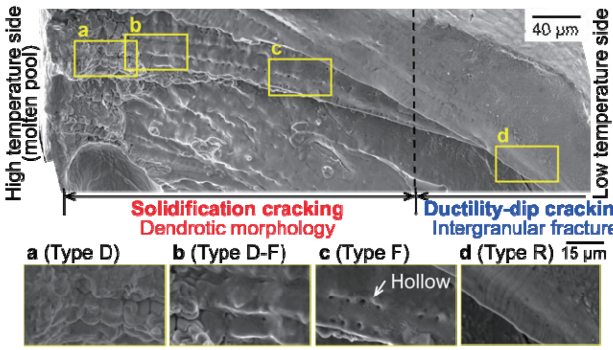

Fig. 3 Fracture surface of hot cracking during LBW at 1.0 m/min. (Augmented strain: 2.8%)

the low temperature side, an intergranular fracture surface is observed in Fig. 3d. The presence of hollows is considered proof of SC [7], so the region from the high-temperature side to where the holes exist is identified as SC and the region of intergranular fracture is identified as DDC. In addition, it is confirmed that DDC combines with SC along the temperature gradient in this type of hot cracking.

Figure 4 shows the number of SC and total crack lengths in LBW and GTAW. Both values saturate at about 2.0% of augmented strain. In addition, both values are much higher when using GTAW than those using LBW. In the case of LBW, a high welding speed tends to decrease both the number of SC and total crack length.

The weld bead width measured at each welding speed (augmented strain of 4.3%) is indicated in Fig. 5. The width of the weld beads produced by GTAW is much higher than those of LBW. Moreover, in the case of LBW, the bead width decreases with increasing welding speed. This difference in weld bead width gives an inaccurate evaluation of SC susceptibility parameters, such as the crack length and crack number: the influence of the bead width should therefore be eliminated to clearly evaluate the effect of welding speed on solidification

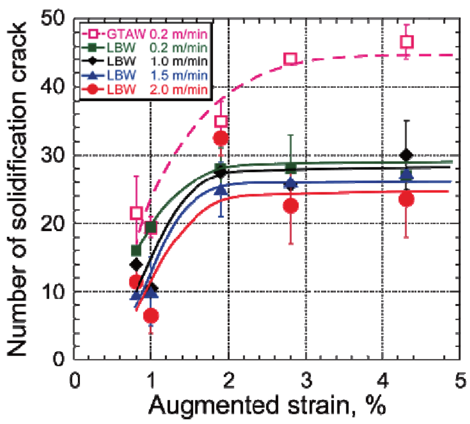

a) Number of SC

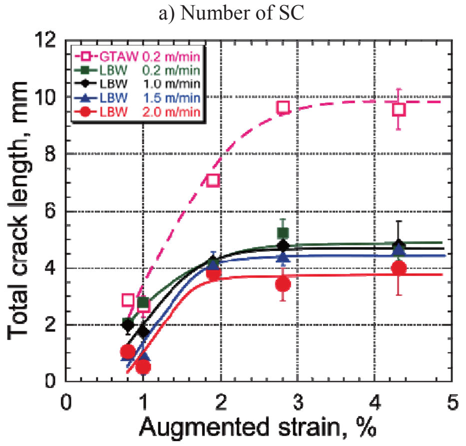

b) Total crack length

Fig. 4 Number of SC and total crack length.

cracking susceptibility.

Figure 6 shows the number of SC and total crack lengths divided by the bead width. Both values are nearly the same for both GTAW and LBW at 0.2 m/min. Increasing the speed of LBW initially increases both the number density of SC and the total crack length per bead width and then these values decrease slightly. The maximum values are obtained at approximately 1.5 m/min. This proves that solidification cracking susceptibility in LBW increases with welding speed up to about 1.5 m/min and

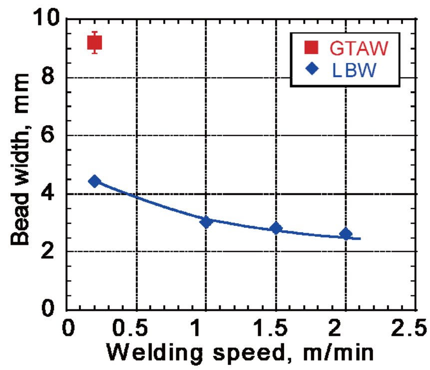

Fig. 5 Bead width for each welding condition. (Augmented strain: 4.3 %).

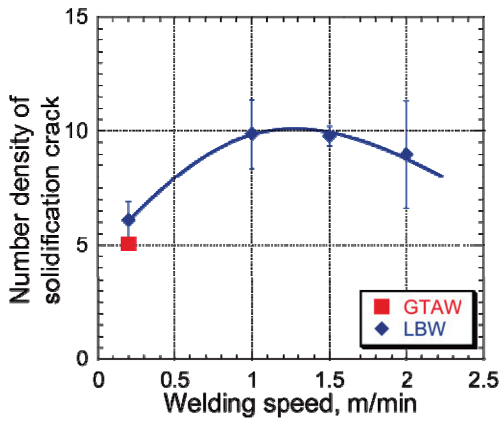

a) Number density of SC

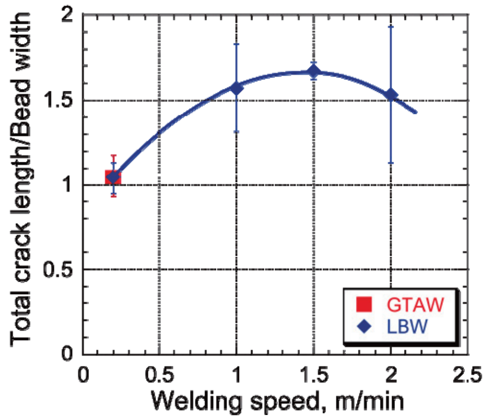

b) Total crack length per bead width

Fig. 6 Number density of SC and total crack length per bead width. (Augmented strain: 4.3 %)

then decreases.

Temperatures were measured by inserting an optical-fiber radiation thermometer into the rear of the molten pool. By synchronizing the timing of the high-speed camera and the fiber thermometer, as shown in Fig. 7, the liquidus temperature was determined by the temperature at which the edge of the molten pool reached the center of the thermometer. The liquidus temperature for LBW at 0.2 m/min is 1383 °C. The average cooling curves for LBW at 0.2 and 1.0 m/min (based on several trials) are indicated in Fig. 8, and the average liquidus temperatures are 1385 °C and 1389 °C, respectively. However, the cooling curves and liquidus temperatures obtained at 1.5 and 2.0 m/min varied widely. It was also difficult to determine the precise time at which the molten pool trail touched the center of the thermometer at higher welding speeds (1.5 and 2.0 m/min) because the rear of the molten pool extended in the opposite direction to the welding direction.

To calculate BTR, the maximum crack length along the direction of heat flow is required. The maximum lengths of centerline cracks at 0.2 and 1.0 m/min are shown in Fig. 9. The maximum centerline crack initiated within 250 μm of the thermometer diameter at the rear center of the molten pool. The centerline crack could also result from a direct contribution of the augmented strain. The saturated lengths are obtained over an augmented strain of 2.0 % and the saturated value at a welding speed of 0.2 m/min is higher than that at 1.0 m/min.

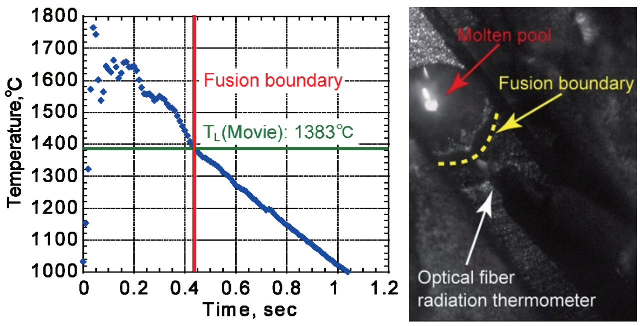

Fig. 7 Temperature measurement during LBW at 0.2 m/min.

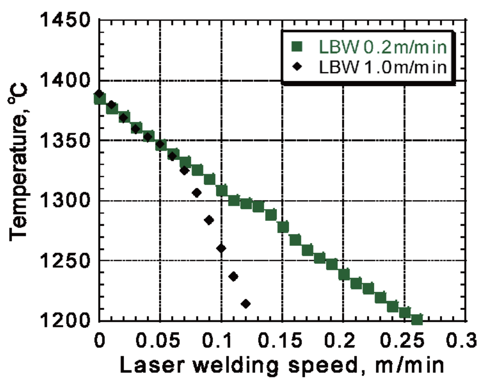

Fig. 8 Average temperature profiles during LBW at 0.2 and 1.0 m/min.

Figure 10 shows ductility curves for LBW at 0.2 and 1.0 m/min. BTR at 0.2 m/min is 79 °C and that at 1.0 m/min is only 11 °C. It is therefore considered that LBW at 0.2 m/min is more susceptible to solidification cracking than LBW at 1.0 m/min. However, the longest SC was initiated at the edge of the rear side of the molten pool at a welding speed above 1.0 m/min, as shown in Fig. 2b. It is therefore difficult to obtain real BTR values using Trans-Varestraint test during LBW at higher welding speeds by applying a conventional temperature measurement method, such as direct insertion of thermometer. A two-dimensional temperature distribution measurement method is required.

4. Conclusions

To evaluate solidification cracking susceptibility of type 310S stainless steel during LBW, cracking morphology and use of Trans-Varestraint test method were investigated. The number density of SC and the total crack length of SC per unit bead width increase first and then decrease slightly with increasing welding speed. Maximum values for both parameters were obtained at welding speeds of approximately 1.5 m/min. In the case of LBW at high welding speed, temperature measurement by direct

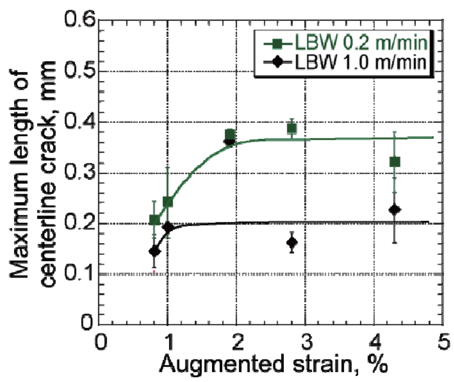

Fig. 9 Maximum length of centerline crack at rear center of molten pool during LBW at 0.2 and 1.0 m/min.

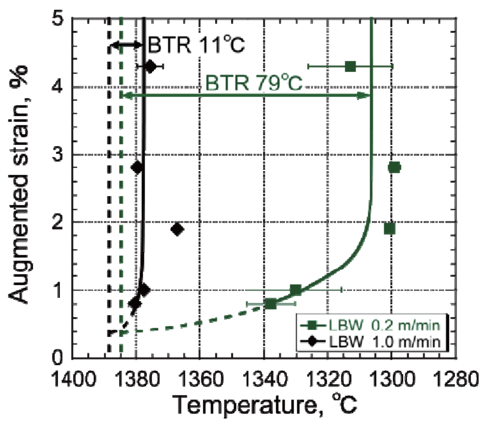

Fig. 10 BTR during LBW at 0.2 and 1.0 m/min.

insertion of a thermometer could be achieved for speeds of 0.2 and 1.0 m/min; however, it was difficult to obtain the temperature profile and liquidus temperature at welding speeds above 1.5 m/min because of extension of the rear side of the molten pool and wide variation of temperature gradient. BTR at 1.0 m/min was less than that at 0.2 m/min during LBW because the longest SC tended to occur at the sides of the molten pool at high welding speeds. To measure the true BTR using the Trans-Varestraint test during LBW at high welding speeds, a two-dimensional temperature distribution measurement method is required.

References

1) K. Kadoi, A. Fujinaga, M. Yamamoto and K. Shinozaki: The effect of welding conditions on solidification cracking susceptibility of type 310S stainless steel during laser welding using an in-situ observation technique, Weld World, 57 (2013), 383–390.

2) S. Ohshita, N. Yurioka, N. Mori and T. Kimura: Prevention of solidification cracking in very low carbon steel welds, Welding Research Supplement, (1983), 129–136.

3) R. Singh: Weld Cracking in Ferrous Alloys, Woodhead Publishing Limited (2009), 409.

4) S. Kou: Welding Metallurgy, John Wiley & Son, Inc (2003), 53–55, 266.

5) E.J. Chun, H. Baba, K. Nishimoto and K. Saida: Development of Varestraint test procedure with laser beam welding – Solidification cracking in laser welds of austenitic stainless steels (Part 1)-, National Meeting of JWS, Japan (2014), 174–175.

6) S. Katayama, T. Fujimoto and A. Matsunawa: Correlation among solidification process, microstructure, microsegregation and solidification cracking susceptibility in stainless steel weld metals, Transactions of JWRI, 14 (1985), 123–- 138.

7) F. Matsuda, H. Nakagawa, S. Ogata and S. Katayama: Fractographic investigation on solidification crack in the Varestraint test of fully austenitic stainless steel –Studies on fractography of welded zone (Ⅲ), Transactions of JWRI, 7 (1978), 59–70.